A Flexible Model to Calculate Buried Cable Ampacity in Complex Environments

G. Callender, K.F. Goddard, J.K. Dix and P.L. Lewin, *Member, IEEE*

***Abstract*—The ampacity of buried cables is significantly influenced by the thermal properties of the burial environment. When these thermal properties are not homogeneous it is usually necessary to utilize simulations with a relatively high computational cost that may also use commercial software. In this paper an alternative approach is proposed using conformal maps. Temperature is calculated in an annular domain which is a conformal mapping of the half plane space. Circumferential dependence is captured by expanding temperature as a Fourier series, a finite difference solver then determines temperature components radially. The model is as flexible as any two-dimensional slice model of heat transfer through thermal conduction only. Two case studies are considered: three land-based cables in planar configuration and a submarine export cable. The thermal properties of both burial environments are based on conditions which may be encountered in the field and exhibit a high level of stratification. Using a finite element analysis simulation as a benchmark, typical percentage differences in cable ampacities were 0.5%-1%. In addition to accuracy and flexibility the low computational cost of the proposed approach allows for large parameter sweeps, which may be required in a design phase, without requiring commercial software.**

Index Terms—buried power cables, heat transfer, conformal mapping, finite element simulation, thermal models

I. Introduction

BURIED high voltage cable systems represent a key component of electrical networks. Power flow capacity is typically thermally constrained such that the conductor temperature does not exceed 90°C to prevent failure of the adjacent electrical insulation [1]. Given that the majority of the temperature rise is due to Joule heating, driven by the load current in the conductor, it is necessary to determine the permissible ampacity of the cable, also referred to as its rating. Determining the temperature rise due to such heating requires the calculation of heat transfer both within the cable and its surrounding environment [2]. The IEC standards provide analytical solutions of temperature, under both static and step load scenarios, for cables buried in thermally homogeneous environments [3, 4]. However, it is often the case that thermally limiting cable sections are not in thermally homogenous environments. An example would be export cables from offshore wind farms, where the thermal conductivity of the burial environment can be highly stratified [5].

Finite element analysis (FEA) has been widely used by the research community to determine cable temperatures in complex environments [6]. However, a downside is that the approach typically requires commercial software. Furthermore, in certain scenarios the computational time associated with running FEA simulations can be prohibitive. Examples include the analysis of large distributed temperature sensing (DTS) datasets or parametric sweeps during a design phase. This had led to the development of approaches which are judged to be sufficiently close to FEA simulations yet are accessible to a wide user base and offer savings in computational cost [7, 8, 9].

In this paper a flexible model for calculating heat transfer from buried cables, and consequently their ampacity, is introduced. The model makes use of conformal maps which have previously been used in the study of the thermal influence of backfill on cables [10]. In this earlier work the conformal transformation mapped the burial environment to a rectangular domain and then approximated the thermal resistance of domains based on their relative areas in the mapped space. The strength of using a conformal transformation is that solutions of the stationary heat equation are unchanged by the mapping. This enables temperature to be calculated in a mapped domain, where the calculation is often simpler. If required, the solution can then be mapped back to the geometry of the burial environment.

The conformal transformation used in this paper maps the burial environment to an annular region; this is advantageous for two key reasons. Firstly, it is conceptually consistent with existing approaches in the literature [11]. Secondly, as heat transfer is predominantly radial in the mapped space circumferential heat transfer can be represented by performing a Fourier expansion. This results in a simple, yet flexible, model which is amenable to a finite difference solver and can be implemented in any standard programming language. The proposed model is tested by comparing against FEA simulations across two case studies of cable systems in environments with heterogeneous thermal properties that are representative of real-world scenarios.

II. Conformal Mapping

The conformal transformations used in this work are Möbius transformations that map the half plane with a circle removed to an annulus centered at the origin. Both geometries are defined in the complex plane. The circle in the half plane is centered at depth B, and is mapped to the inner circle of the annulus with unchanged radius R. The real line in the half plane is mapped to the outer circle of the annulus, which has radius $2\tilde{B}$. Hereafter the inner circle is treated as the cable surface. The real line in z space and the outer circle in w space shall be treated as the ground surface. The relationship between the z and w spaces is shown in Figure 1.

Letting z and w represent complex coordinates in the half plane and annulus respectively the transformations are as follows

$$z = x + jy = j\gamma \frac{w - 2j\tilde{B}}{w + 2j\tilde{B}} \tag{1}$$

$$w = u + jv = -2\tilde{B}j \frac{z + j\gamma}{z - j\gamma} \tag{2}$$

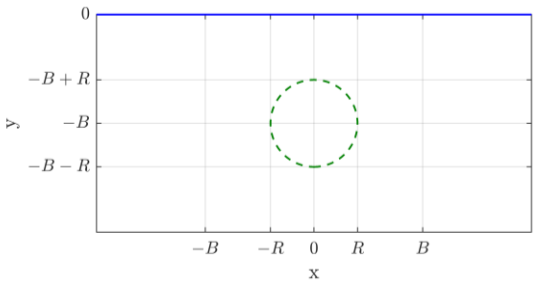

(a) z Half Plane Space

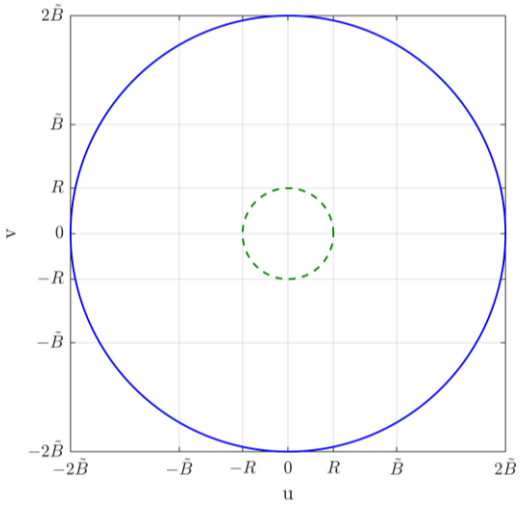

(b) w Annulus Space

Fig. 1. Demonstration of the conformal mapping between the (a) z and (b) w spaces. The solid blue and dashed green lines in (a) are mapped to the corresponding lines in (b) and visa versa. Note that the plot of the half plane in (a) is truncated for clarity; the half plane in its entirety is mapped to the annulus.

To make the radius of the cable in both spaces to be equal to R requires,

$$\gamma = \tilde{B}\left(1 - \frac{R^2}{4\tilde{B}^2}\right), \tag{3}$$

and, for the hole to be centered at $z = -jB$ requires,

$$\tilde{B} = \frac{B + \sqrt{B^2 - R^2}}{2}, \tag{4}$$

The stationary form of the heat equation with no heat sources, and with heat transfer due to thermal conduction only, is

$$\vec{\nabla} \cdot \vec{q} = 0, \qquad \vec{q} = -k\vec{\nabla}\theta \tag{5}$$

where $\vec{q}$ is the heat flux, k is the thermal conductivity and θ is the temperature. In a region of fixed thermal conductivity (5) is a Laplace equation for temperature θ, the solution of which is unchanged under a conformal transformation. This property can be exploited to solve for temperature in a simple geometry which is a conformal transformation of a more complex geometry where it is desired to calculate temperature.

A simple example that admits an analytical calculation would be to consider a case where the cable and ground surface are both isotherms and the thermal conductivity of the cable surroundings is a homogenous value k. In the w space this problem is easily solved in cylindrical coordinates centered on the origin, as there is no circumferential dependence on temperature. The temperature can be calculated as follows

$$\theta(r) = \theta_G + (\theta_C - \theta_G)\frac{\log r - \log 2\tilde{B}}{\log R - \log 2\tilde{B}}. \tag{6}$$

where $r = \sqrt{u^2 + v^2}$. (6) can then be used to show

$$\theta_C = qT_4 + \theta_G \tag{7}$$

where

$$q = -2k\pi R\frac{d\theta}{dr}|_{r=R} \tag{8}$$

is the total amount of heat leaving the cable surface and T_4 is the full form of the external thermal resistance of a single isolated buried cable in the IEC 60287-2 standards [12]. The conformal transformation (2) can then be used to map the temperature solution, (6), to the half plane as shown in Figure 2 which is representative of the real-world installation conditions of a cable. It is of interest to note that in both spaces the isothermal contours are circular, but they are only concentric in the annular space. A property of Möbius transformations is the mapping of circles and straight lines to circles and straight lines [13].

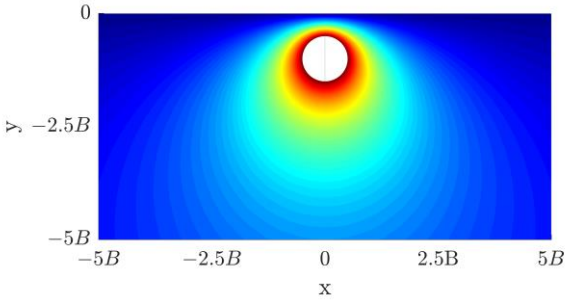

(a) z Half Plane Space

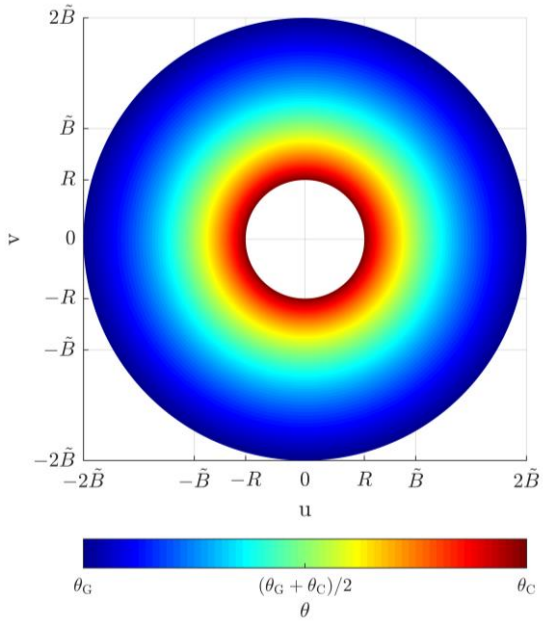

(b) w Annulus Space

Fig. 2. Figure showing temperature in (a) z and (b) w spaces. The cable surface is set to θ_C, the ground surface is set to θ_G. The analytical calculation to determine temperature is performed in the w space.

III. Cable Thermal Model

For many cable circuits the system may be significantly more complex than a single isolated cable buried in a thermally homogeneous environment. In this section a flexible thermal model is introduced that can capture significant inhomogeneities in the thermal properties of the burial environment. The section begins with the simplest case of a continuous load, i.e. a stationary problem, for a single isolated cable. The model is developed to consider a dynamic scenario for a single buried cable and finally multiple buried cables. Only conductive heat transfer is considered in this approach, convective and radiative heat transfer will introduce additional terms into the governing equation for temperature, capturing these processes is beyond the capability of the model presented in this paper.

A. Continuous Load Model for an Isolated Buried Cable

In keeping with the simple example of the previous section, temperature will be solved for in the annular w space. However, circumferential dependence of temperature is now possible due to inhomogeneous soil thermal conductivities, which would lead to non-concentric isotherms. Temperature and thermal conductivity in the w space may be written as a Fourier series

$$\theta(r,\phi) = \sum_{n=-\infty}^{\infty} \theta_n(r) e^{jn\phi} \tag{9}$$

$$k(r,\phi) = \sum_{m=-\infty}^{\infty} k_m(r) e^{jn\phi} \tag{10}$$

where ϕ is the polar angle orientated anticlockwise with respect to the positive u axis and θ_n and k_m are radially dependent complex Fourier coefficients. It should be noted that although these coefficients are complex θ and k are real which means that

$$\theta_n = \theta^*_{-n},\ k_m = k^*_{-m}. \tag{11}$$

k_m can be determined by mapping the thermal conductivity in the z space, where it is a known function of x and y, into the w space, where it is a function of r and ϕ. $k_m(r)$ can then be calculated as

$$k_m(r) = \frac{1}{2\pi}\int_0^{2\pi} k(r,\phi) e^{-jm\phi}\ d\phi. \tag{12}$$

Figure 3 shows an example of the thermal conductivity in the half plane space, thermal conductivity in the mapped space, and the Fourier expansion of the thermal conductivity truncated at third order terms. The use of a truncated Fourier series will result in thermal conductivities that under and overshoot the true values in the mapped space. It is possible that for very large differences in thermal conductivities, over an order of magnitude, negative values of thermal conductivity could occur. This was not an issue in any of the burial environment thermal conductivities used in this work which are based on real world measurements [14-17]. In the unlikely event that negative values of thermal conductivity did occur they could be removed by increasing the order of the Fourier expansion or manually adjusting values making conservative assumptions.

In order to determine temperature it is necessary to solve for θ_n in the annulus space. The static form of the heat equation, (5), in cylindrical coordinates is

$$\frac{1}{r}\frac{\partial}{\partial r}\left(rk\frac{\partial\theta}{\partial r}\right) + \frac{1}{r}\frac{\partial}{\partial\phi}\left(\frac{k}{r}\frac{\partial\theta}{\partial\phi}\right) = 0 \tag{13}$$

$$\frac{k}{r}\frac{\partial\theta}{\partial r} + \frac{\partial k}{\partial r}\frac{\partial\theta}{\partial r} + k\frac{\partial^2\theta}{\partial r^2} + \frac{1}{r^2}\frac{\partial k}{\partial\phi}\frac{\partial\theta}{\partial\phi} + \frac{k}{r^2}\frac{\partial^2\theta}{\partial\phi^2} = 0 \tag{14}$$

(9) and (10) are truncated at a specified order N and then substituted into (14). Distinct powers of $e^{jn\phi}$ can then be isolated resulting in $2N+1$ coupled governing equations for the real and imaginary parts of θ_0 to θ_N, note that θ_0 is by definition purely real. To avoid the need for internal boundary conditions within the burial environment, the thermal conductivity is expressed as a smooth function using logistic curves in the half plane space. The gradient of the curve was set to 1000 m^{-1} for all case studies considered, the model results were insensitive to the exact value provided the transition between distinct domains occurred at sufficiently small length scales. Logistic curves with a coarser gradient, 20 m^{-1}, are used in Figure 3 for clarity.

The governing equations for the different coefficients in radial coordinates are solved using a second order central finite difference scheme. For all cases considered in this work the cable surface and the ground surface are considered as isotherms with no circumferential dependence. As such the boundary conditions for the burial environment thermal model are

$$\theta_0(r = R) = \theta_{\mathrm{C}} \tag{15}$$

$$\theta_0(r = 2\tilde{B}) = \theta_{\mathrm{G}} \tag{16}$$

$$\theta_n\left(r = R \text{ or } r = 2\tilde{B}\right) = 0 \text{ when } n \neq 0. \tag{17}$$

However, it should be noted that this is not a restriction of the model; spatially dependent temperature or heat flux boundary conditions could be applied if required. The use of an isothermal cable surface allows a standard thermal ladder network to be used to model the cable interior.

B. Dynamic Load Model for an Isolated Buried Cable

When transient loads are considered the heat equation now reads

$$C_{\mathrm{v}}\frac{\partial\theta}{\partial t} + \vec{\nabla}\cdot\vec{q} = 0 \tag{18}$$

where C_{v} is the volumetric heat capacity, which may be spatially dependent. The total thermal mass of the burial environment should remain the same under the mapping. Formally

$$\int C_{\mathrm{v}\,z}\ dA_z = \int C_{\mathrm{v}\,w}\ dA_w. \tag{19}$$

Conformal maps do not conserve area, the relationship between area elements is

$$dA_w = J dA_z \tag{20}$$

where J is the Jacobian determinant of the transformation [13]. It follows that

$$C_{\mathrm{v}\,w} = \frac{C_{\mathrm{v}\,z}}{J}. \tag{21}$$

J may be written as

$$J = \frac{\partial u}{\partial x}\frac{\partial v}{\partial y} - \frac{\partial v}{\partial x}\frac{\partial u}{\partial y} = \left|\frac{dw}{dz}\right|^2 \tag{22}$$

where the variables are defined as in (1) and (2). Differentiating (2) and (1),

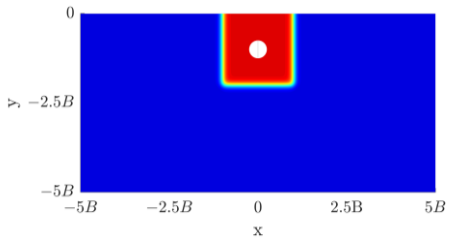

(a) z Half Plane Space

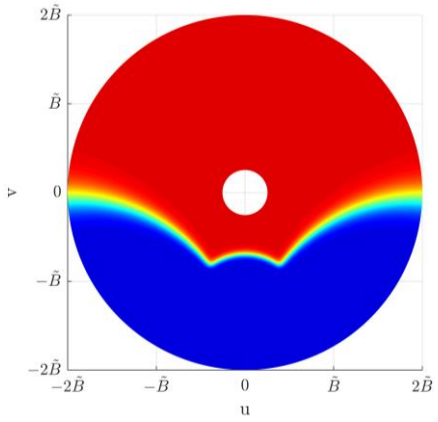

(b) w Annulus Space

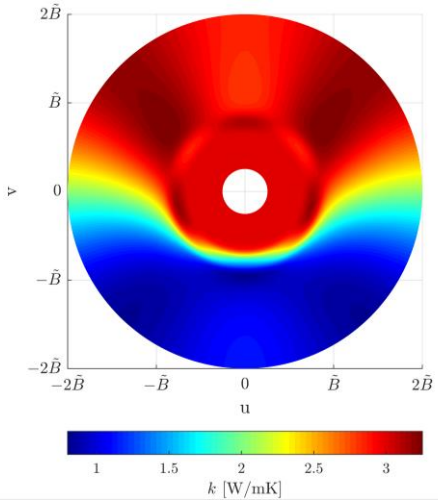

(c) w Annulus Space

Fig. 3. Thermal conductivity as a function of position in: (a) z space and (b) w spaces. (c) is a Fourier expansion of the thermal conductivity in w space truncated at third order terms. Note that the plot of the half plane in (a) is truncated for clarity; the half plane in its entirety is mapped to the annulus. Logistic curves with a gradient of 20 m^{-1} are used to smooth the transition between regions of different thermal conductivity.

$$\frac{dw}{dz} = -2\tilde{B}j\left(\frac{1}{z-j\gamma} - \frac{z+j\gamma}{(z-j\gamma)^2}\right) = \frac{-4\gamma\tilde{B}}{(z-j\gamma)^2} \tag{23}$$

$$\frac{dz}{dw} = j\gamma\left(\frac{1}{w+2j\tilde{B}} - \frac{w-2j\tilde{B}}{\left(w+2j\tilde{B}\right)^2}\right) = \frac{-4\gamma\tilde{B}}{\left(w+2j\tilde{B}\right)^2}. \tag{24}$$

Combining these results with (22),

$$J = \frac{16\,\gamma^2\,\tilde{B}^2}{(|z-j\gamma|^2)^2} = \frac{16\,\gamma^2\,\tilde{B}^2}{(x^2+(y+\gamma)^2)^2} \tag{25}$$

$$J = \frac{\left(|w+2j\tilde{B}|^2\right)^2}{16\,\gamma^2\,\tilde{B}^2} = \frac{\left(u^2+v^2+4\tilde{B}^2+4\,v\,\tilde{B}\right)^2}{16\,\gamma^2\,\tilde{B}^2} \tag{26}$$

The Jacobian determinant calculated using (25) is plotted in Figure 4.

It can be clearly seen from (25) that J tends to zero as the distances from the cable becomes large and, through (21), this results in exceptionally large values of $C_{v\,w}$. When expressed as a truncated Fourier series this can result in unphysical negative values in the mapped space. To avoid this issue the volumetric heat capacity in the annular domain is instead set to

$$C_{v\,w} = \frac{C_{v\,z}}{\tilde{J}}. \tag{27}$$

where

$$\tilde{J}(u,v) = \min(\beta, \max(J(u,v), 1/\beta)) \tag{28}$$

β is a positive constant that is determined iteratively such that the volumetric heat capacity, calculated through (27), is always positive. The use of reciprocal limits is appropriate, as $J \sim 1$ in the vicinity of the cable and this is the location where it is most crucial to use accurate values of volumetric heat capacity. Initially β is set to 1 and then increased in powers of 2 until negative values of the Fourier expansion are observed. It is then reset to its previous value. The value of β will be dependent on the truncation order. Typical thermal ladder networks of buried cables, which also solve for heat transfer in an annular space, do not consider this scaling of the volumetric heat capacity [11]. The approach proposed here is comparable to adjustments made to thermal capacitances of the soil made by Lux and co-authors [8].

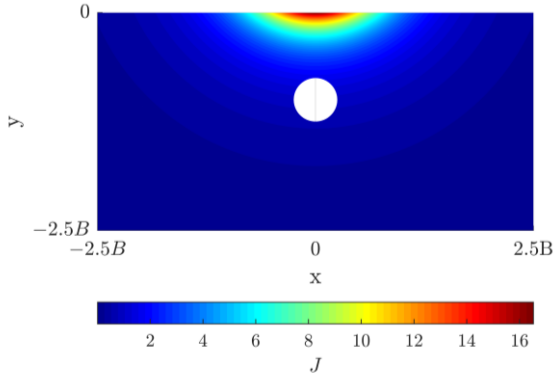

Fig. 4. The Jacobian determinant J in the z half plane space, $B = 1$ and $R = 0.25$.

The governing equations for the different temperature coefficients are then solved using backwards Euler time stepping and a second order central finite difference scheme in space.

C. *Dynamic Load Model for Multiple Buried Cables*

In the case of multiple buried cables the impact of mutual heating may be significant. However, for a given cable of interest it is unnecessary to consider the thermal properties of surrounding cables when quantifying the impact of mutual heating, provided the cable separation is large in relation to its radius. Using this result, and the fact that the heat equation, (18), is linear, it is possible to solve for the temperature of each cable independently adding on the temperature rise above ambient at a given cable location due to the surrounding cables when calculating the temperature dependent heat sources. This same assumption is made when

calculating the impact of mutual heating in the IEC standards [4]. Other than considering the temperature dependency of the heat sources the temperature of each cable can be calculated in isolation.

IV. Case Studies

In this section two case studies are considered that are not amenable to the current methodology in the IEC 60287 standards using the conformal mapping finite difference (CM FD) approach introduced in the previous section. A comparison is made against an equivalent finite element analysis (FEA) model. The thermal model of the cable interior for the CM FD models is a standard RC thermal ladder network. A schematic of the network for the cable of an armored cable is provided in Figure 5.

For cases with multiple cables the conformal mapping approach calculates the temperature in cable interior for each cable sequentially following the approach described in Section III C. An important point is that, although they are not considered here, the conformal mapped model is adaptable to non-isothermal cable surfaces and ground surfaces, the consideration of which may be required in some cases [9]. The approach is as flexible as any two-dimensional finite element simulation of heat transfer by thermal conduction. Furthermore, for the implementation and cases studies considered in this report, the run time of all CM FD models is at least an order of magnitude lower than the equivalent FEA models. This is of significant value when analyzing operational data [7] or when calculating real time thermal ratings (RTTR) [8]. The ratings calculations undertaken here are intended as a comprehensive test of model performance.

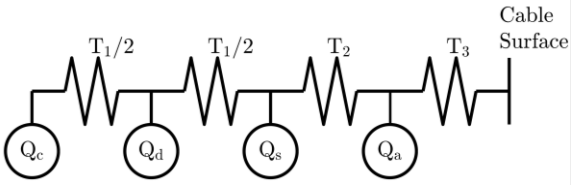

Fig. 5. Schematic of the cable thermal network model for an armored cable. Heat sources from the conductor Q_c, dielectric Q_d, sheath Q_s and armour Q_a are taken from the IEC standards [3].

A. Planar Cables with Layered Soils

Brownfield (ex-industrial) sites are frequently re-purposed for the location of the onshore substations that support offshore windfarms. These environments are characterized by highly heterogeneous materials into which the cable has to be buried. A typical burial stratigraphy would be “made ground” (remnants of the previous infrastructure material), modern soils and bedrock. In this example the three cables have been laid in a planar configuration in 1 m of sand (2 W/mK [14]), that overlies the local bedrock (Mudstone – 1.75 W/mK [15]) but is overlain by 2m of made ground. In this scenario the made ground is an extreme coal based slag, 0.33 W/mK [16], but typical cement based products would consistently have thermal conductivities below 1 W/mK [17]. The distribution of the thermal conductivities in both the “real” half plane and mapped spaces is shown in Figure 6 for the central cable, it should be noted that the distribution will be dependent on the cable under consideration.

The three cables are located within a sand filled layer in a planar configuration at a depth of 2.5 m, below the “Made Ground” within the sand layer. They are a 400 kV design with Milliken conductors and cross bonded sheaths. The cable separation is 200 mm. This means that three independent CM FD thermal simulations are performed, one per cable, as per the methodology introduced in Section III C.

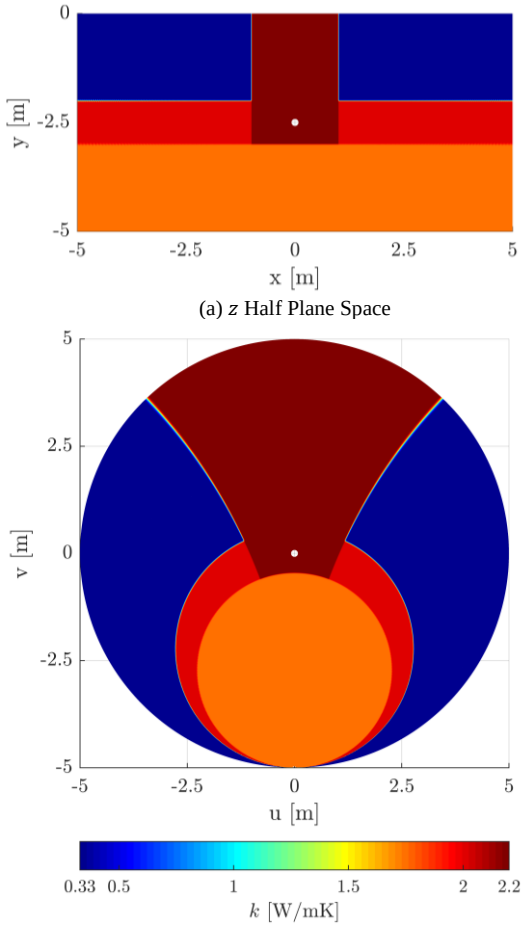

(a) z Half Plane Space

(b) w Annulus Space

Fig. 6. Thermal conductivity as a function of position in: (a) z space and (b) w spaces for the central cable. Note that the plot of the half plane in (a) is truncated for clarity; the half plane in its entirety is mapped to the annulus. The burial environment consists of three distinct layers: 2m Made Ground k =0.33 W/mK, 1m Sand k =2 W/mK and the remainder is Mudstone k =1.75 W/mK. The cables are laid in a trench with stone dust backfill, k =2.2 W/mK, which extends to the ground surface.

It is informative to observe the thermal conductivity distribution in the mapped space in order to make judgements on the relative importance of the distinct soil layers. In some scenarios this could even be used to provide justification for neglecting certain soil layers if it is clear visually they will have a negligible thermal impact in the mapped space. In this case study the horizontal lines in the half plane space are all mapped to circles which meet at the base of the annulus space ($u = 0, v = -2\tilde{B}$). The “Made Ground” is clearly the largest area within the mapped space and so it is expected to make a significant difference to the heat transfer within the burial environment. Conversely the sand layer, despite being within the immediate vicinity of the cable outside of the trench, is less important.

The continuous rating for a Summer (15°C ambient) and Winter (5°C ambient) season have been sourced from the UK Met Office and represent the 2019 Mean Summer Air Temperature (15.1°C) and Mean Winter Air Temperature (5.2°C). A full convergence study was performed adjusting the number of finite difference nodes, referred to as L, and the Fourier series truncation order N. For a given N, L was increased starting from 250 by powers of two until the difference in the continuous rating between calculations was

less than 0.1%. N was then increased in steps of 1 until the difference in the rating was also 0.1%. In this case convergence was achieved at $N = 5$ $L = 500$, the corresponding FEA node count was 16879. It can be clearly seen in Figure 7 that the error decreases with increasing N as the expanded Fourier series is a more accurate representation of the true thermal conductivity distribution. Comparing against FEA simulations the error was 0.5% for the summer and winter continuous ratings.

The use of conformal maps also allows the temperature distribution within the burial environment to be determined, not just the cable temperature. A comparison is made in Figure 8. It can be clearly seen that the conformal approach is able to capture the temperature distribution around the cables including the steeper temperature gradients within the upper soil layer which are present due to its high thermal resistivity. If greater accuracy was desired the truncation order could be increased, or, alternatively, a fully two-dimensional model could be used to solve for temperature in the annulus space. Although this would be of comparable computational cost to FEA it is likely preferable for some users as the annular space easily allows the use of uniformly distributed grids.

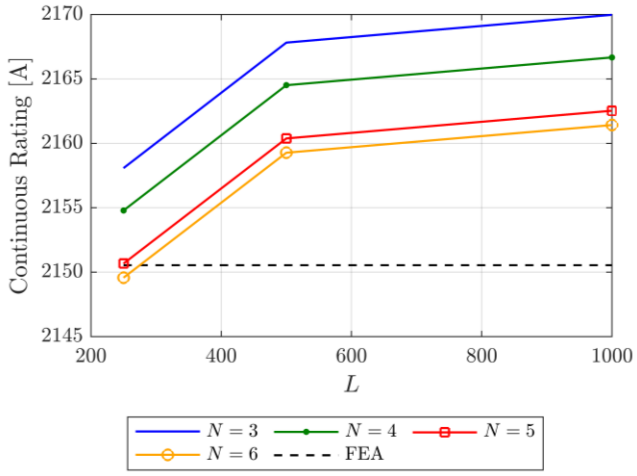

Fig. 7. Comparison of the continuous rating calculate using FEA (dashed line) and the conformal mapping finite difference method for different truncation orders (N) and finite difference node counts (L). As the truncation order increases the conformal mapping method becomes closer to the FEA solution. It is a coincidence that the lower node count results in a lower error when compared to FEA.

In addition to continuous ratings the 6h and 24h short term ratings have been determined at a range of pre-fault levels. These durations and pre-fault levels are typical for cable systems [18]. A full comparison is provided in Table 1. The highest error is 1.4% over all considered combinations.

TABLE I
6H AND 24H RATINGS FOR PLANAR CABLES IN LAYERED SOILS

Season	**Preload**	**Rating [A]**			
		6h		24h	
		CM FD	FEA	CM FD	FEA
Summer 15°C	75%	3188	3230	2626	2645
	60%	3605	3655	2863	2887
	30%	4093	4151	3149	3178
Winter 5°C	75%	3411	3456	2807	2828
	60%	3857	3911	3061	3086
	30%	4379	4442	3365	3397

While realistic it should be noted that the thermal conductivity variation is extreme, with a difference of nearly an order of magnitude between the soil domains. As such this case study should be seen as a "stress test" of the model, requiring a high truncation order to the Fourier expansions to achieve an accurate result. In the next case study a less significant variation is considered which allows for accurate calculations at a lower truncation order.

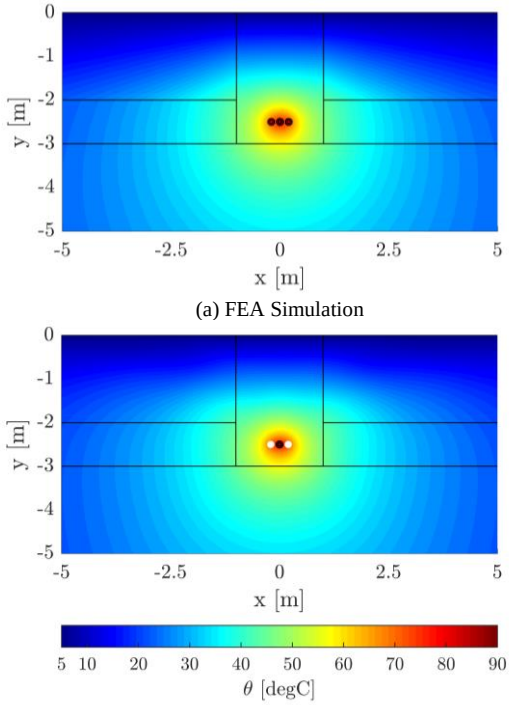

(a) FEA Simulation

(b) CM FD Simulation

Fig. 8. Temperature surfaces of three cables in a planar configuration in layered soils for the winter continuous rating: (a) FEA simulation and (b) CM FD Simulation.

B. Export Cable at Landfall in Layered Marine Sediments

Cables shallowly buried on the continental shelf, whether connecting offshore renewable energy resources or trans-national interconnectors frequently experience highly stratified marine sedimentary sequences. For mid- to high-latitude shelves this is the consequence of the complex interplay of terrestrial and marine geological processes over the last few hundred thousand years. The cable design in this example is based on a 3 phase AC windfarm export cable, and has been used in previously published work [7]. It is buried at -1.25m, in the center of a 0.5 m thick peat layer (0.8 W/mK) which is overlain by 0.5 m of quartz sands (2.2 W/mK) and 0.5 m of silts (1.2 W/mK) and rests upon a mudstone bedrock (1.45 W/mK) [14]. The thermal conductivity distribution in both the "real" half plane space and the mapped spaces is shown in Figure 9. Seasonal ambient temperatures for the continuous ratings are set to 15°C for Summer and 10°C for Winter as these are typically used for cable rating in NW Europe [19].

A convergence study was performed in an identical fashion to the previous case study. Convergence was achieved at a far lower truncation level, $N = 4$. This is as expected due to the relative similarities of the thermal conductivities of the burial environment which vary significantly less than the order of magnitude differences in the previous study. This means that the isotherms in the annulus space will be closer to the typical concentric distribution, and any variations from this can be captured using at a relatively low truncation order. The errors,

compared to FEA calculations, were also lower with errors of 0.2% for both the summer and winter continuous ratings. A surface plot of temperature within the burial environment is provided in Figure 10.

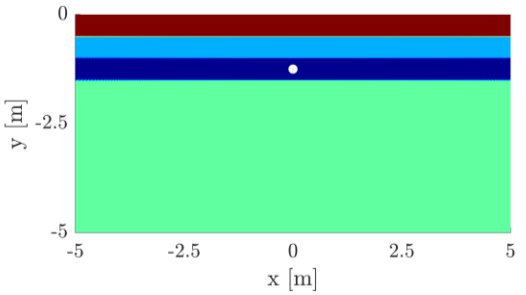

(a) z Half Plane Space

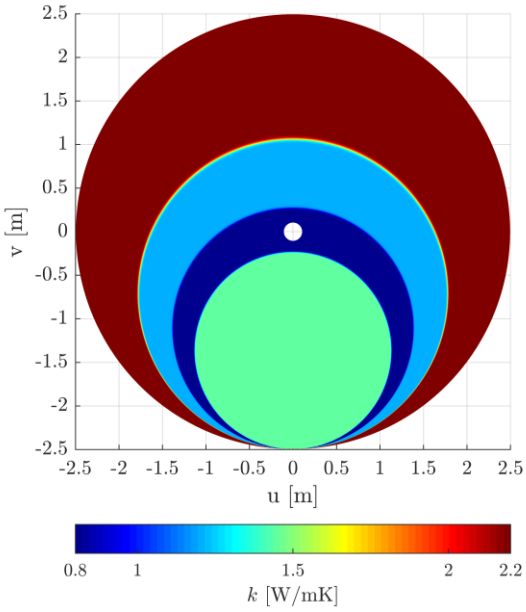

(b) w Annulus Space

Fig. 9. Thermal conductivity as a function of position in: (a) z space and (b) w spaces for the central phase. Note that the plot of the half plane in (a) is truncated for clarity; the half plane in its entirety is mapped to the annulus. The burial environment consists of four distinct layers: 0.5m Quartz Sands k =2.2 W/mK, 0.5m Silt k =1.2 W/mK, 0.5m Peat k =0.8 W/mK and the remainder is Mudstone k =1.45 W/mK.

Short term ratings for the export cable system have also been calculated, the results are provided in Table 2. The largest error between the calculations was 0.4%.

TABLE II
6H AND 24H RATINGS FOR EXPORT CABLE IN LAYERED MARINE SEDIMENTS

Season	Preload	Rating [A]			
		6h		24h	
		CM FD	FEA	CM FD	FEA
Summer 15°C	75%	1157	1153	992	990
	60%	1269	1265	1049	1048
	30%	1401	1395	1118	1117
Winter 10°C	75%	1198	1194	1026	1025
	60%	1314	1309	1085	1084
	30%	1450	1444	1156	1155

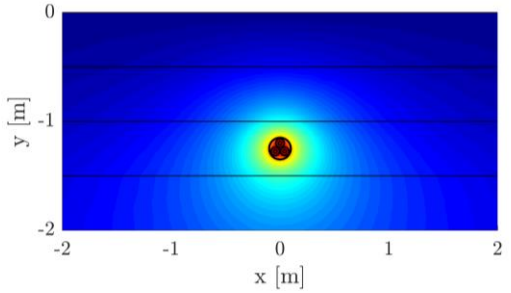

(a) FEA Simulation

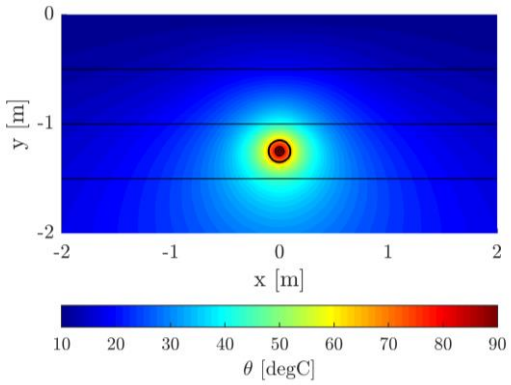

(a) CM FD Simulation

Fig. 10. Temperature surfaces of export cable in layered sediments for the winter continuous rating: (a) FEA simulation and (b) CM FD Simulation. The CM FD simulation uses a thermal network model for the cable with a single equivalent power core.

V. CONCLUSION

This paper has introduced a flexible low computational cost model for conductive heat transfer in complex burial environments using conformal maps which does not require commercial software. The approach has been validated against two case studies of buried cable systems with thermally inhomogeneous soil layers using finite element analysis simulations as a benchmark. Both continuous and short-term ratings were calculated. The highest observed error in the ampacity was 1.4%, with typical errors in the range of 0.5%-1%. For the case studies considered in this report, the run time of all CM FD models is an order of magnitude lower than the equivalent FEA models. This is of significant value when analyzing operational data [7] or when calculating real time thermal ratings (RTTR) [8]. The use of conformal maps also allows informative judgements to be made on the relative importance of domains with differing thermal properties on cable temperatures.

Future work could consider non-isothermal cable surfaces which would require angular dependent terms within the cable thermal network model. This may be necessary to achieve the desired accuracy when the thermal properties in the immediate vicinity of the cable surface are circumferentially dependent. An obvious example would be when an export cable makes landfall and is located at the bottom of a thermally resistive pipe.

VI. REFERENCES

[1] G. J. Anders, Rating of Electric Power Cables in Unfavourable Thermal Environments, Hoboken, NJ: John Wiley & Sons Inc, 2005.

[2] F. De Wild and a. et, "A guide for rating calculations of insulated power cables," in *Jicable*, Versailles, 2015.

[3] *Electric Cables – Calculation of the Current Rating*, IEC, 60287-1-1:2006, 2006.

[4] *Calculation of the cyclic and emergency current rating of cables*, IEC60853-3, 2002.

[5] J. A. Pilgrim, S. Catmull, R. D. Chippendale, R. Tyreman and P. L. Lewin, "Offshore wind farm export cable current rating optimisation," in *Offshore 2013*, Frankfurt, Germany, 2013.

[6] F. De León and G. J. Anders, "Effects of Backfilling on Cable Ampacity Analyzed With the Finite Element Method," *IEEE Transactions on Power Delivery*, vol. 23, no. 2, pp. 537-543, 2008.

[7] G. Callender, D. J. Ellis, K. F. Goddard, J. K. Dix, J. A. Pilgrim and M. Erdmann, "Low Computational Cost Model for Convective Heat Transfer from Submarine Cables," *IEEE Transactions on Power Delivery (Early Access)*, 2020.

[8] J. Lux, T. Czerniuk, M. Olschewski and W. Hill, "Non-concentric Ladder Soil Model for Dynamic Rating of Buried Power Cables," *IEEE Transactions on Power Delivery (Early Access)*, 2020.

[9] S. Purushothaman, F. de León and M. Terracciano, "Calculation of cable thermal rating considering non-isothermal earth surface," *IET Generation, Transmission & Distribution*, vol. 8, no. 7, p. 1354–1361, 2014.

[10] CIGRE, "The calculation of the effective thermal resistance of cables laid in materials having different thermal resistivities," *Electra*, vol. 98, p. 19–42, 1985.

[11] M. Diaz-Aguiló, F. De León, S. Jazebi and Terracciano, "Ladder-Type Soil Model for Dynamic Thermal Rating of Underground Power Cables," *IEEE Power and Energy Technology Systems Journal*, vol. 1, pp. 21-30, 2014.

[12] *Electric Cables – Calculation of the Current Rating*, IEC 60287-2-1:2006, 2006.

[13] H. Cohen, Complex Analysis with Applications in Science and Engineering, New York: Springer, 2007.

[14] J. K. Dix, T. J. Hughes, C. J. Emeana, J. A. Pilgrim, T. J. Henstock, T. M. Gernon and C. E. L. Thompson, "Substrate controls on the life-time performance of marine HV cables," in *SUT Offshore Site Investigation and Geotechnics (OSIG) 8th international conference, 'Smarter Solutions for Future Offshore Developments'*, London, 2017.

[15] D. Banks, J. G. Withers, G. Cashmore and C. Dimelow, "An overview of the results of 61 in situ thermal response tests in the UK," *Quarterly Journal of Engineering Geology and Hydrogeology*, vol. 46, no. 3, pp. 281-291, 2013.

[16] J. M. Herrin and D. Deming, "Thermal conductivity of US coals," *Journal of Geophysical Research: Solid Earth*, vol. 101, no. B11, pp. 25381-25386, 1996.

[17] J. C. Mendes, R. R. Barreto, A. C. B. de Paula, F. P. da Fonseca Elói, G. J. Brigolini and R. A. F. Peixoto, "On the relationship between morphology and thermal conductivity of cement-based composites," *Cement and Concrete Composites*, vol. 104, p. 103365, 2019.

[18] R. Huang, J. A. Pilgrim and P. L. Lewin, "Dynamic Cable Ratings for Smarter Grids," in *4th IEEE PES Innovative Smart Grid Technologies Europe (ISGT Europe)*, Copenhagen, 2013.

[19] CIGRE Working Group B1.35, *A guide for rating calculations of insulated cables.*, CIGRE, 2015.

VII. Appendix

MATLAB code for conformal mapping finite difference (CM FD) simulations has been made available on IEEE Xplore.

VIII. Biographies

George Callender was born in Basildon, UK in 1991. He received M.Sci (Hons) in Natural Sciences (Maths and Physics) from the University of Durham, UK in 2013. He received a Ph.D. degree in electrical engineering from the University of Southampton, UK in 2018. He is currently a Research Fellow in High Voltage Numerical Modelling at the University of Southampton. His research interests include partial discharge phenomena and the thermal modelling of high voltage plant.

Kevin F. Goddard received a BSc in Electrical Engineering from University of Southampton, England in 1982. He obtained his PhD in 1992 for work on stray fields in the stator frames of electrical machines, also from University of Southampton.

After short periods in industry, he became a Research Fellow at University of Southampton. He worked on electromagnetic design and numerical modelling of electrical machines. His recent work involved electromagnetic and thermal modelling in cables. Dr. Goddard is a member of the IET.

Justin K. Dix is Head of the Geology and Geophysics Research Group at the University of Southampton, Southampton, U.K. His major interests are the use of high-resolution geophysical and geological techniques to investigate the quaternary history of and modern sedimentary process operating on the continental shelf.

Prof. Paul L. Lewin (M'05-SM'08-F'13) was born in Ilford, Essex in 1964. He received the B.Sc. (Hons) and Ph.D. degrees in electrical engineering from the University of Southampton, UK in 1986 and 1994, respectively. He joined the academic staff of the University in 1989 and is Head of Electronics and Computer Science, where he is also Director of the Tony Davies High Voltage Laboratory. His research interests are within the generic areas of applied signal processing and control. Within high voltage engineering this includes condition monitoring of HV cables and plant, surface charge measurement, HV insulation/dielectric materials and applied signal processing. Since 1996 he has received funding and grants in excess of £30M, supervised 47 graduate students to successful completion of their doctoral theses and published over 500 refereed conference and journal papers in these research areas. He is a Chartered Engineer, a Fellow of the IET, and former president of the IEEE Dielectrics and Electrical Insulation Society.